Journal of Design Against Fatigue

https://minerva-aset.com/jdaf/

Comparison of energy absorption in conventional and auxetic shoes: gait analysis and finite element modeling

Mahdi Daei Daei, Amir Nourani*, Mohammadmahdi Honarmand

Department of Mechanical Engineering, Sharif University of Technology, Azadi Ave., Tehran, Iran

P A P E R I N F O

Paper history:
Received 20 July 2023
Received in revised 4 August 2023
Accepted 5 August 2023

Keywords:
Auxetic; Finite Element (FE) modeling; gait analysis; strain energy; shock absorption

A B S T R A C T

A three-dimensional finite element (FE) model of the heel and shoe sole was developed to analyze the effects of materials with different Poisson's ratios for midsole on energy absorption and impact shock in the heel area during walking. The heel model was obtained from CT-scan data. The FE model was verified using Anybody software for barefoot with data obtained from gait analysis. Sole layers and plantar soft tissue were modeled, and five different Poisson's ratios (-0.4, -0.2, 0, 0.2, and 0.4) were compared for the midsole layer. In order to obtain the contact force, experiments were performed on a force plate using shoes with either auxetic or conventional midsole layer. Rayleigh damping theory was used to simulate viscous damping behavior in the midsole layer. The results showed that for materials with the same Young's modulus, there was less compression, energy absorption, and viscous dissipation energy in the auxetic model in comparison to the conventional model. However, when compressive strains of sole layers were the same (i.e., by changing Young's modulus), more energy absorption (about 9%) was observed for the midsole with negative Poisson's ratio with respect to the conventional midsole layer. The outcome of this work can guide shoe manufacturers to design shoe soles with longer lifetime that, at the same time, cause less fatigue for the spine.

1. INTRODUCTION

Frequent impact loadings of the musculoskeletal system during locomotion in case of not being effectively damped have the potential to lead to several injuries and health problems, such as stress fractures, osteoarthritis, cartilage breakdown, Type 1 shin splints, knee injuries, and low back pain [1]. Attenuating the impacts between the foot and the ground during gait is one of the most important functions of a footwear sole. It has been shown that both ground reaction forces and transient stress waves transmitted up the lower limb during walking were affected by footwear. Furthermore, midsoles with stiffer materials were generally associated with higher shock levels transmitted up to spine [2]. Hence, choosing the main material for the shoe sole, as one of the most effective parameters determining the whole sole characteristic, has always been addressed by footwear manufacturers. Natural rubber, polyurethane, polyvinyl chloride (PVC), and ethylene-vinyl acetate (EVA) foams are some materials commonly used as the main material of the footwear sole. In the past few years, the idea of using soles with "auxetic structures" has been patented by some manufacturing companies [3]. Auxetic structures have a negative Poisson's ratio, ν, defined as the ratio of transverse strain to longitudinal strain. A vast range of artificial auxetic materials have been developed in different scales [4]. The auxetic structures might be varied between a few nanometers to 1 meter [5]. These structures are fabricated either by 3D printing or by post-processing the existing non-auxetic foams [6]. 3D printing is considered as a novel methodology in manufacturing the auxetic structures with non-random cell orientation, however, high cost, scale limitation, and the existence of defects are among the technical barriers of this method [7]. An example of post-processing the conventional foams is implementing the thermo-mechanical methodology which includes compressing the foam along three orthogonal directions during molding [8]. As a result of this methodology, polyvinyl chloride (PVC) foam [9,10], closed-cell PU foam [11] and silicone rubber foam [12] could be converted into foams with auxetic behavior. The mechanical properties of these foams can be adjusted by applying different geometrical and processing parameters in the thermos-mechanical procedure [13]. Lakes and Elms [14] performed some holographic indentation tests and proved that auxetic re-entrant foams had a higher yield strength and lower stiffness, E, in comparison to conventional foams of the same density. Moreover, they found that dynamic impact energy absorption was noticeably higher for auxetic re-entrant foam than that for conventional foams. Moroney and Alderson [15] conducted a study on improving the protection of sports apparel using an auxetic material. The enhanced

*Corresponding Author Email: nourani@sharif.edu (Amir Nourani)

Please cite this article as: Mahdi Daei Daei, Amir Nourani, Mohammadmahdi Honarmand, Comparison of energy absorption in conventional and auxetic shoes: gait analysis and finite element, ***Journal of Design Against Fatigue,*** Vol. 1, No. 02, (2023), 43-51

properties of the apparel were conformability, superior energy absorption, and reduced thickness. Also, more flexibility was felt by users due to the synclastic curvature in the deformed auxetic material. Experiments on auxetic foams in snow- sport safety devices carried out by Allen and Duncan [16] showed that the energy absorption of a composite pad with auxetic foam was about three times of the energy absorption of a conventional equivalence under quasi-static compression with a concentrated load. Having a high energy absorption capacity and simultaneously high indentation resistance, which is generally associated with better stability, would make an auxetic material a suitable fit for the footwear sole [17]. It was also shown in Ref [18] that using an auxetic material in high heels would decrease the peak plantar pressure onto the forefoot in comparison to that of traditional materials. Their study focused only on the redistribution of plantar loafing in forefoot, and not in the heel area, during walking. Ref. [19] patented a new sport shoe design with auxetic sole that was claimed to aid conformability around heel area. Furthermore, an auxetic heel support designed by [20] was shown to be more comfortable and shock absorptive compared to bulk elastomers and foams. Dehaghani et al. [21] went even further and showed a decrease of impact in lumbar spine by wearing an auxetic shoe compared to the conventional shoes in a set of gait analyses. Although the auxetic materials may be a sufficient alternative of conventional materials for sports shoes, the amount of viscous dissipation energy in auxetic materials in comparison to the conventional counterparts is still unidentified. None of the studies mentioned above suggested a model of shoe midsole interacted with an auxetic structure. No study obtained the amount of viscous dissipation energy caused by compression in the shoe sole. This study aimed to generate a finite element (FE) model of an auxetic midsole to obtain the amount of energy absorption and comfortability in comparison to traditional midsoles and to measure the efficiency of using this midsole. Several experiments were performed on a force plate using shoes with auxetic and non-auxetic midsoles to compare the impact shocks during walking. Moreover, viscous energy loss, as an important factor in designing the shoe sole, was calculated for both types of midsole.

2. MATERIAL AND METHODS

2.1. GAIT ANALYSIS

In clinical gait analysis, both the individual abilities to walk and how he walks are studied. Instrumented gait analysis is an accurate and precise measurement tool to capture the human gait parameters such as spatiotemporal, kinematic, and kinetic measures [22]. In contrary with wearable sensing systems, gait measurement tools are low-cost, low setup-time, lightweight and portable [23]. In this study, the heel impact and energy absorption in the rear section of the shoe sole were analyzed. The gait analysis with auxetic and three non-auxetic (i.e., conventional) shoes was carried out on a Kistler force plate in Mowafaghian Rehabilitation Institution, Tehran, Iran, to obtain the normal forces created during walking. The force-time diagrams were obtained, and the measured forces were input to the FE model as tabular data to obtain the heel load and stresses in both auxetic and regular structures. An adult male subject weighted 71.8 kg with a height of 175 cm, walked on a force plate, wearing either the conventional or auxetic shoes (see Figure 1). The thickness of all soles in the heel area was around 2.5 cm, and all of them had the same size of 42.5 (European standard). The auxetic shoe (i.e., with the auxetic midsole) was the Nike product (Nike free RN with model number: 408323), and three non-auxetic shoes were conventional sports shoes from different brands. The subject was asked to walk at a steady pace, beginning at least 5 meters ahead of the force plate starting point. The experiments on each pair of shoes were repeated five times to ensure the repeatability of testing.

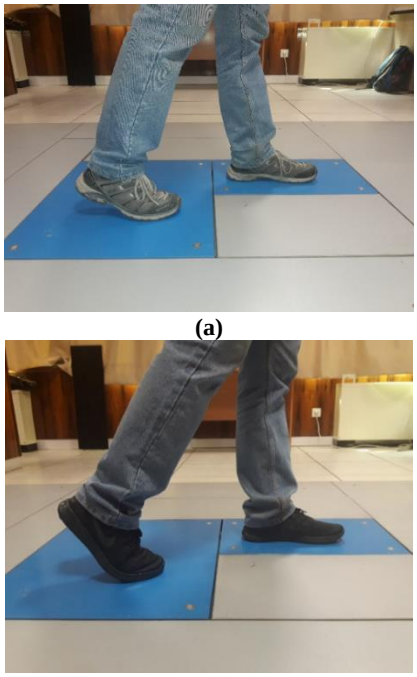

Figure 1 (a) Walking on the force plate with a conventional shoe. (b) Walking on the force plate with Nike auxetic shoe. All the experiments were performed by a subject, who weighted 71.8 Kg with a height of 175 cm.

2.2. FINITE ELEMENT MODELING

In order for modeling the heel, the calcaneus from a male adult was generated by a CT scan (see Figure 2a). The point cloud data extracted from CT-scan was then converted to a solid body using SOLIDWORKS 2017 to build the bone geometry. Finally, the model was imported in ABAQUS 2016 (Figure 2b). The calcaneus bone was assumed to be elastic. Table 1 lists the mechanical properties used in the model. The plantar soft tissue was placed under the calcaneus (Figure 2c). In order to avoid extra simulation costs, only the part of the plantar soft tissue which contacts the shoe sole was modeled. Plantar soft tissue was modeled as an extruded surface covering the calcaneus. The geometry of the surface was defined based on the contact surface between the foot and shoe. The minimum unloaded thickness of the tissue, from the bottom of the tissue to the lowest part of the calcaneus, was reported 15.2 mm (see Figure 2c) [24]. The experimental compressive stress-strain diagram of plantar soft tissue was used to estimate the hyper-

elastic behavior of the tissue [25]. Ogden fitting criteria was used to estimate the hyper-elastic behavior. The sole of the shoe usually consists of three layers: insole, midsole, and outsole. In modern sports shoes, insole and midsole layers are made of EVA foam to be lighter and more flexible than conventional foams [26]. Generally, the outsole is made of carbon rubber or blown rubber. These materials were modeled as linear elastic (Table 1) since FE results proved that in low strains, e.g., strains experienced in sole layers during walking, there was no meaningful difference between elastic and hyper-elastic model. The geometry of the sole was modeled the same as the cross-section of the plantar soft tissue model with a thickness of 2.5 cm (Figure 2d). The upper part of the sole is insole, with a thickness of 2 mm [26]. The midsole was placed under the insole with the properties of an EVA foam but different in the amount of Poisson's ratio: EVA foam has the Poisson's ratio of almost zero, while in the present model, Poisson's ratio was varied from -0.4 to 0.4. Under the midsole, the outsole was modeled with a thickness of 2 mm [26]. In the FE model the part geometries were assembled together by rigid tie connection (from top to bottom: calcaneus, plantar soft tissue, and shoe sole). The calcaneus was assumed fixed by ENCASTRE constraint (constraint on all displacements and rotations at a node) on the side of ankle and the other parts were free to move in the space. A rigid plate was placed at the bottom of the sole to simulate the real boundary conditions during walking. The obtained impact loads from the force plate will be applied to this rigid plate. Due to its complex geometry the model was meshed with quadratic tetrahedral elements with the size of 2 mm and the mesh convergence analysis was performed. Prony series were used to simulate the viscoelastic behavior of the midsole with the coefficients [27] listed in Table 2.

Table 1. Material properties used in FE models.

Model part	Young's modulus (MPa)	Poisson's ratio	Mass density (kg/m^3)
Calcaneus [28]	7300	0.3	812
Soft plantar tissue [20]	Hyper-elastic	-	1052
Insole [24]	5.4	0.49	200
Midsole [24]	10	variable	200
Outsole [27]	25	0.42	1100

Table 2. Prony coefficients of viscoelastic behavior in the midsole; gi Prony is the shear relaxation or shear traction relaxation modulus ratio, ki Prony is the bulk relaxation or normal traction relaxation modulus ratio, and tau Prony is the relaxation time.

g-i Prony	k-i Prony	tau-i Prony
0.195	0.195	0.91

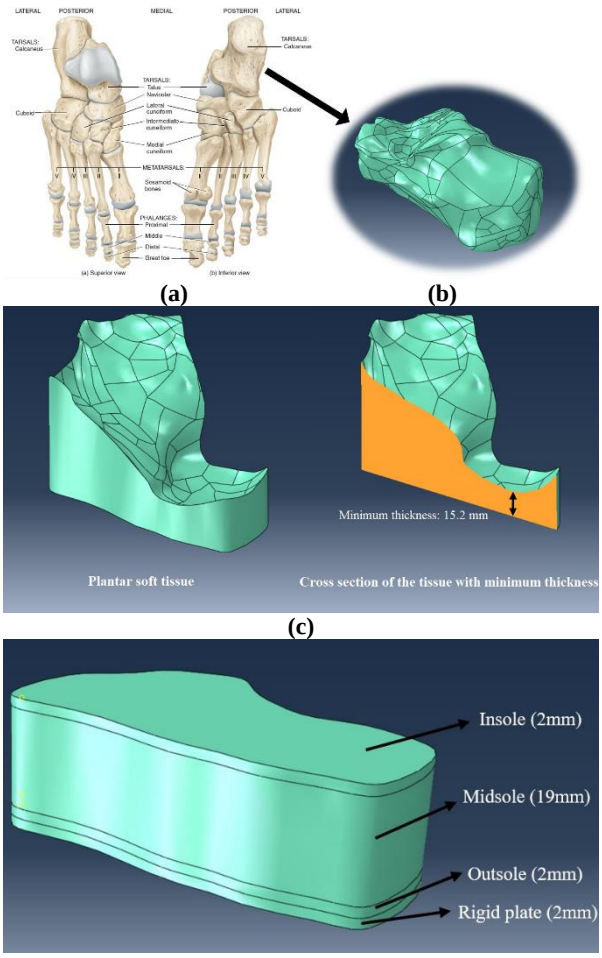

Figure 2 (a) Skeleton of the foot consists of tarsal bones, including talus and calcaneus [28]. (b) Imported calcaneus bone model in ABAQUS from point cloud provided by a CT-scan. (c) Plantar soft tissue under the calcaneus covered the lower surface of the calcaneus. (d) The sole

2.3. Modal Analysis to obtain viscous damping parameters

Rayleigh damping theory was used to simulate viscous damping behavior in the midsole [29]. The equivalent Rayleigh damping form is:

$$[C] = \alpha[M] + \beta[K] \quad (1)$$

where [C], [M], and [K] are the damping, mass and stiffness matrices of the system, respectively. α and β are damping coefficients defined as [29]:

$\beta = \frac{2\xi_1\omega_1 - 2\xi_m\omega_m}{\omega_1^2 - \omega_m^2}$	(2)
$\alpha = 2\xi_1\omega_1 - \beta\omega_1^2$	(3)

where ξ_1 = damping ratio for the first mode of the system; ξ_m = damping ratio for the mth significant mode; ω_1 = natural frequency for the first mode of the system, ; ω_m = natural frequency for the mth significant mode. Modal analysis was carried out on the sole to find the damping coefficients required to simulate the viscoelastic behavior of the sole. For such a system with large degrees of freedom, approximately 100% of mass participation was found to occur in the first modes [29]. Hence, the goal was to find these modes and then to obtain the damping coefficients. A modal analysis was performed on the midsole in SOLIDWORKS 2017 simulations. Boundary conditions were applied so that the lateral side of the midsole was fixed in the XZ plane (see Figure 3) (i.e., it was assumed that the lateral side of the midsole did not move during walking in XZ plane). Mesh sizes were exactly the same as those in the ABAQUS model. Different Poisson's ratios (0.4, 0.2, 0, -0.2, and -0.4) were applied in the model to obtain the Rayleigh damping coefficients in each simulation. It was found that about 97% of mass participation occurred in the first four modes of the model with ν = 0.4 (Table 3). It was assumed that the Rayleigh damping coefficients of the current shoe sole were approximately the same as those of the natural rubber. For this model, the minimum damping ratio, ξ_1=0.02 was assigned to the first mode, and the specified damping ratio of ξ_4=0.08 was defined for the fourth mode [30], which are the values for a natural rubber. The modal analysis for the models with other Poisson's ratios (i.e., 0.2, 0, -0.2, and -0.4) also confirmed that significant modes were the first four modes. As mentioned above, m was 4 for the present study. By substituting the values obtained from modal analysis (see Table 3) in Eq. (2) and Eq. (3), α and β were calculated. The same procedure was done to obtain α and β for other Poisson's ratios (as can be seen in Table 4), and corresponding Rayleigh coefficients were defined for the midsole with different values of Poisson's ratio.

Table 3 Results of the modal analysis of midsole with Poisson's ratio of 0.4 in SOLIDWORKS.

Mode number	Natural frequency (rad/s)	Mass participation Y direction (%)
1	6878	85.260
2	8539	0.148
3	10525	0.923
4	10926	10.402
5	12773	0.003
6	14454	0.005
7	15735	0.000
8	15867	0.005

Table 4. Rayleigh coefficients obtained for different Poisson's ratios

Poisson's ratio	ω_1	ω_4	ξ_1	ξ_4	α	β *10^{-6}
0.4	6878	10926	0.02	0.08	-691.85	20.43
0.2	7068	11949	0.02	0.08	-593.97	17.55
0	7205	12787	0.02	0.08	-519.13	15.55
-0.2	7564	13882	0.02	0.08	-507.51	14.15
-0.4	8279	15560	0.02	0.08	-521.14	12.43

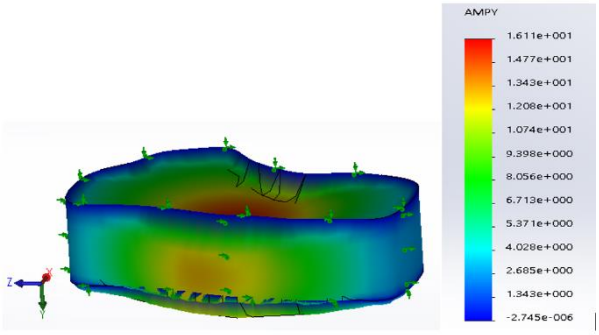

Figure 3 Modal analysis of midsole in SOLIDWORKS (mode 1 for the model with ν = 0.4). The lateral side of the midsole was fixed in the XZ plane.

In order to obtain stresses on the ankle and, consequently, the impact force, it was assumed that the upper side of the calcaneus was fixed with the load acting on the lower side of the sole (Figure 4a). Corresponding impact loads acting under the rigid plate were the measurements from the force plate, as described in Section 2.1. It will be shown in Section 3 that two peaks were observed in the force-time graph obtained from the force plate in gait analysis. The first peak was attributed to the load experienced by the heel, while the second one was related to the toe-off moment. Since the heel stresses are investigated in this study, only the first peak was applied in the FEM; i.e., the load data from beginning to the time of the first peak using a tabular amplitude were input to the model. Since the load was distributed on the sole area, it was defined as a pressure to the bottom side of the model (see Figure 4a). The simulations were done for five different values of Poisson's ratio (0.4, 0.2, 0, -0.2, and -0.4) and their corresponding damping coefficients obtained from Table 4 (α and β). The explicit solver in Abaqus 2016 was implemented on a 4-core 2.40 GHz processor with 8 Gb of memory and each simulation took around 10 hours.

2.4. VERIFYING THE FE MODEL

In order to verify the FEM, an experiment by a barefoot male subject with a weight of 83 kg and a height of 174 cm was performed on the force plate. Normal forces measured on the

force plate (Figure 5a) were input to the barefoot FE model (i.e., the shoe sole layers were removed from the model). Vertical reaction forces were obtained during impact. These forces were the loads transferred from the calcaneus to the ankle at the beginning of the impact when the heel touched the ground. Anybody software was then used to obtain the forces created in the ankle during walking. The gait model in Anybody was defined with the weight and height of the person (Figure 5b). Similarly, the vertical forces created in the ankle in the gait model had two peaks; the first one attributed to the heel interaction with the ground. Figure 5c compares the force data in the ankle from the start of walking to the moment of the first peak in FEM and Anybody model. The timing was slightly different in these models due to the difference in walking speed between the experiment and Anybody model. The graphs were scaled in the same time period to eliminate this timing difference. The normalized root-mean-square deviation formula was used to obtain deviation between two sets of data with the calculated normalized error of 8.8 %. Therefore, it was concluded that the magnitude of forces and behavior of force-time graphs obtained from Anybody software and FEM were approximately the same during the time of walking. Moreover, the peak loads on the heel were almost equal for both models.

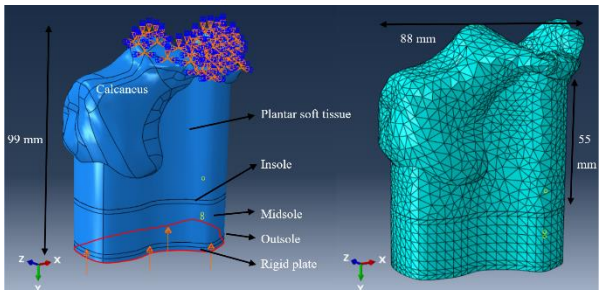

(a) **(b)**

Figure 4 The boundary conditions and load applied to the FE model. The calcaneus was fixed on the side of the ankle. Loading extracted from the force plate was applied as pressure to the lower side of the rigid plate. (b) The model was meshed into tetragonal elements with global size of 4 mm.

3. RESULTS AND DISCUSIONS

A comparison of measured force-time graphs for auxetic and regular shoes is shown in Figure 6; the auxetic graph shows the average data of 5 experiments with the same shoes and the same conditions to minimize the effects of human errors and make the comparison less dependent on the manner of walking. The conventional graph shows the average value of three sets of experiments, which were done with three different conventional shoes (again, each set of experiments with each pair of shoes was repeated five times). The vertical forces are those created during walking in the lower side of the sole. The two force-time graphs for auxetic and regular midsoles were scaled in the same time period (see Figure 6). Figures7a, 7b and 7c indicate the viscous dissipated energy, strain energy and vertical component (i.e. perpendicular to the sole surface) of mean strain, respectively, for a Young's modulus of 10 MPa with different values of Poisson's ratio. Figure 7d shows the strain energy of an auxetic model with a Poisson's ratio of -0.4 for varying Young modulus values. This negative value for Poisson's ratio was chosen as an example in order to find the mean strains experienced by an auxetic shoe and to compare the results with the outputs obtained from a conventional shoe with the same structure but having a Poisson's ratio of 0.4. The same procedure can be performed for any other value of Poisson's ratio to obtain a set of parameters that can result in same amounts of mean strain.

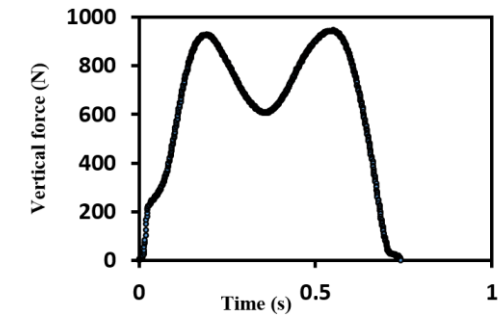

(a)

(b)

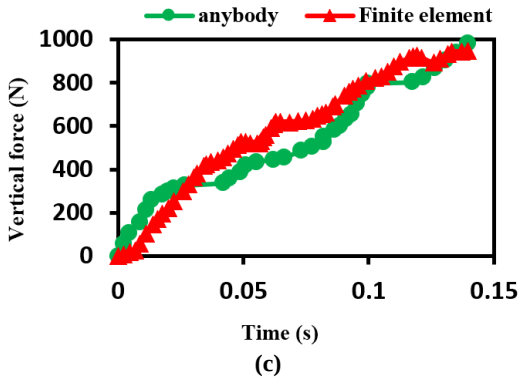

(c)

Figure 5 (a) Vertical force-time graph measured on the force plate for a barefoot male subject with a weight of 83 Kg. (b) Gait model of the examiner walking on the force plate in Anybody software. (c) Comparison between vertical forces created in the ankle of the gait model in Anybody from zero to time of the first peak and forces created in the fulcrum (i.e., the upper side of the calcaneus which assumed to be fixed) in the FE model.

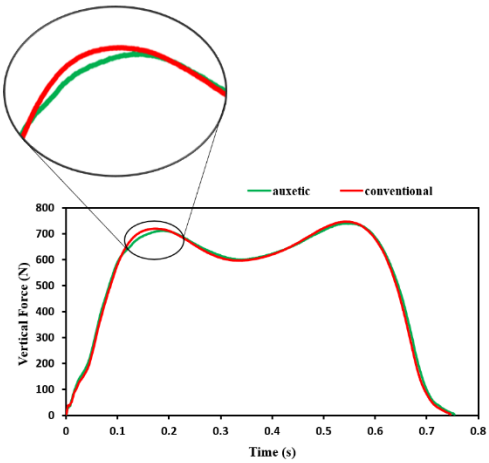

Figure 6 Vertical force-time graph for auxetic and conventional shoes. The curve of conventional midsole is the average of all three conventional shoes.

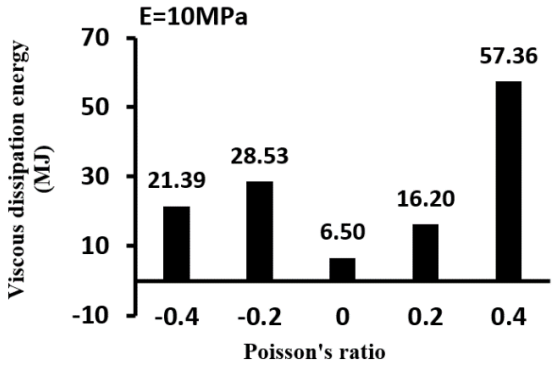

(a)

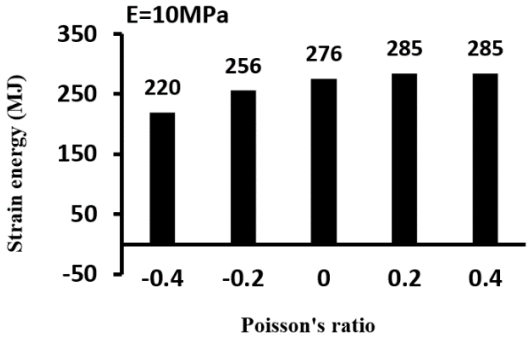

(b)

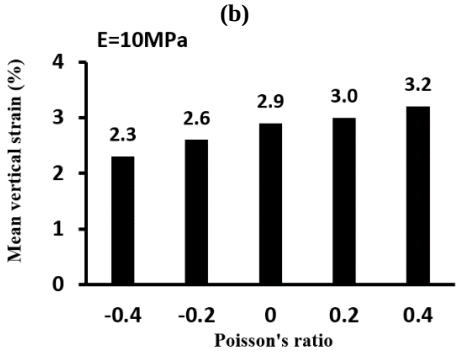

(c)

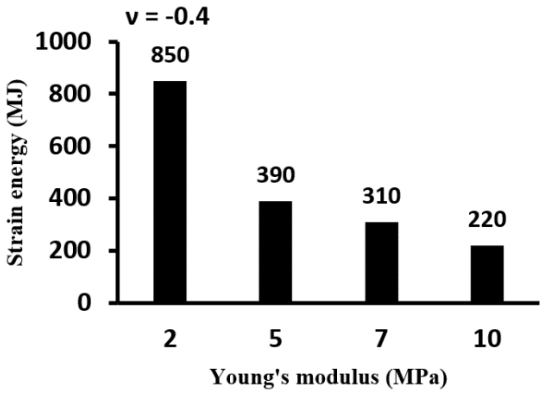

(d)

Figure 7 Viscous dissipation energy for models with different Poisson's ratios and Young's modulus of 10 MPa. (b) Strain energies of sole for models with different Poisson's ratios. The Young's modulus of all models is 10 MPa. (c) The mean value of the vertical strain created in the midsole during compression for models with different Poisson's ratios and Young's modulus of 10 MPa. (d) Strain energies of the auxetic model with Poisson's ratio of -0.4 for different values of Young's modulus.

As seen in Figure 6, the second peak of the force was almost the same in both auxetic and conventional shoes. The first maximum value of force in the auxetic shoe was only about 1.2% less than that in conventional shoes. Moreover, the time of the first peak was delayed in the auxetic shoe about 0.03 s with a decreased slope in force-time graph. Statistical analysis of the two sets of data in Figure 6 yielded the P-value of 0.870, and the difference is statistically insignificant. In Figure 7a, the amount of viscous dissipation energy indicates the energy retrieval capacity of the sole; more viscous dissipation energy means less energy is recovered by the expansion of the sole during separating from the ground. In a mass-spring-damper equivalent system, this energy is the same as the energy eliminated by the damper. It is obvious that the minimum dissipation energy value occurred for $\nu = 0$, while the maximum amount was observed for $\nu = 0.4$. In conclusion, the model with $\nu = 0$ is the most efficient one because it yields less dissipation energy in comparison to other models. As discussed in the introduction, the amount of strain energy reflects the effect of the midsole structure on the heel force; more strain energy means the more energy would be absorbed by the sole, rendering the impact shock decreases. According to Figure 7b, strain energy increases as ν becomes positive. For positive ratio values, there were not any significant changes in strain energy values, implying that a model with $\nu = 0$ had approximately the same capacity to save the strain energy with a material with $\nu = 0.4$. But for the negative values of Poisson's ratio, the strain energy decreased by about 20% with a reduction in Poisson's ratio from $\nu = 0$ to $\nu = -0.4$. The results obtained by assuming the same Young's modulus in all the models contradict the experimental results where the auxetic shoe showed almost more capability to save strain energy and decrease the impact load indicated in Figure 6. In order to investigate this behavior, the mean value of the vertical strain created in the midsole during compression and deformation was calculated. As can be seen in Figure 7c, the mean vertical strain value for $\nu = 0.4$ was about 39% more than that for $\nu =$

-0.4, implying more compression in the midsole for the positive value at the constant Young's modulus of 10 MPa. Finally, a comparison of energies for constant mean strains but varying Poisson's ratios and Young's modulus values was conducted. One way to increase the capacity of stored strain energy is to use a softer material as the midsole; however, Robbins and Waked [31] proved that using a stiffer material in the shoe sole would provide more stability for the user. In other words, more compression in the sole layers might make the user feel unstable. That is why shoe manufacturers do not produce very soft shoe soles. In order for equalizing the mean vertical strain for both auxetic and non-auxetic models, Young's modulus of the midsole in FEM was reduced from 10 MPa to 7 MPa for $\nu = -0.4$. The mean vertical strain obtained was 0.32, the same amount as the mean vertical strain for the model with $\nu = 0.4$ and E = 10 MPa (see Figure 7c). The strain energy obtained from the model with $\nu = -0.4$ and E = 7 MPa was 310 MJ, which was about 9% more than the value obtained from the model with $\nu = 0.4$ and E = 10MPa (Figure 7b). More energy absorption results in a smoother impact during running, as indicated in Figure 6 in the first peak where the heel contacts with the ground. The auxetic shoe shows a lower value of contact force compared to the conventional shows. Nevertheless, the viscous dissipation energy was 72 MJ (i.e., about 26% more than the value of the conventional model with E = 10 MPa and $\nu = 0.4$). Hence, in the auxetic model with $\nu = -0.4$ and E = 7 MPa, there was about 26% more energy loss than the conventional model with E = 10 MPa and $\nu = 0.4$. Strain energies of the auxetic model ($\nu = -0.4$) with different Young's modulus values are shown in Figure 7d. As a result, the strain energy in the auxetic model could increase even more than the conventional model by reducing Young's modulus when the mean vertical strain, and consequently, the sole compression remained unchanged (i.e., without any change in the stability of the user). Therefore, auxetic midsole properties could be optimized to save more strain energy with respect to the strain energy stored by conventional midsoles. More stored strain energy would cause the impact shock to be smoother, and the user would feel more comfortable. Moreover, by bending auxetic foams, a dome-shape curvature is obtained in controversy with saddle shape, which is obtained in conventional foams [17]. This characteristic of auxetic foams would make the midsole cover all the parts of the foot during walking, and the user would feel less resistance when shoes start bending. It was shown that there is a growth in viscous dissipation for the softer model (e.g., in the auxetic model with $\nu = -0.4$ and E = 7 MPa), and it would cause more energy loss during walking. However, for impact shock reduction, it is worthy to use auxetic structure in midsole manufacturing. This model can also be compared with EVA foam (i.e., the foam with Poisson's ratio of zero), which is widely used in shoe sole production in recent years. It is predicted that the auxetic midsole would have better energy absorption (see Figure 7b), while EVA foam would cause less energy loss due to less viscous dissipation energy (see Figure 7a).

4. CONCLUSIONS

This study showed about 9% more energy absorption and less impact shock in the auxetic midsole in comparison to conventional midsoles with the same compression (i.e., the same stability and softness felt by the user) during walking. By reducing Young's modulus from 10 MPa to 7 MPa for the auxetic foam, a higher energy absorption (i.e., an increase of about 41%) was obtained. Hence, with the same amount of softness, higher energy absorption (and subsequently higher comfortability) was achieved. In conclusion, decreasing Young's modulus up to a specific value would not cause more compression in the auxetic midsole in comparison with conventional midsoles. This auxetic characteristic helps the shoe manufacturers to increase the comfort and at the same time keep their softness standards (e.g., the sole should not be too soft in a way that keeping the balance during walking seems though). Furthermore, the fact that the auxetic shoe absorbs considerably higher amount of energy can be beneficial for sport shoe manufacturers who search for recycling the lost strain energy in each step. For an auxetic model, more energy loss (i.e., about 26%) was observed with respect to a conventional model in the most severe case (e.g., an auxetic shoe with Poisson's ratio of -0.4 and Young's modulus of 7 MPa compared to a conventional shoe with Poisson's ratio of 0.4 and Young modulus of 10 MPa). Nevertheless, since the amount of energy loss was much smaller than the amount of energy absorption, it is still recommended to use auxetic structures for shoe sole manufacturing. This work has presented a novel approach to compare the conventional shoe soles with the auxetic ones which enhances the comfort and efficacy. The finite-element approach enabled us to explore different material properties among auxetic materials with low cost and rapid implementation. The latter might be used to optimize the material properties by finding the best configurations for Young modulus and Poisson's ratio. Nevertheless, the feasibility of fabricating such an optimized material remains a question which we leave it for the future works. On the other hand, gait analysis was proven to be a robust tool to obtain the impact force of different types of shoes. In conclusion, the Auxetic foam would be an appropriate alternative for conventional midsole materials in terms of reducing the impact shock transferred to the heel, thereby decreasing the risk of spinal injuries in the long-term. The methodology presented in this work can guide shoe manufacturers to design an optimized structure based on different criteria defined by shoe experts.

5. ACKNOWLEDGMENTS

The authors are grateful to Prof. Farzam Farahmand and Dr. Saeed Behzadipour, faculty members of the Department of Mechanical Engineering at Sharif University of Technology, and fellows from Mowafaghian Rehabilitation institution for their valuable advice and technical support. The assistance of Hossein Korani, a BSc student at Sharif University of Technology, for the experiments is appreciated.

6. REFERENCES

1. R. S. Goonetilleke, Footwear cushioning: Relating objective and subjective measurements, Hum. Factors. 41(2) (1999) 241–256, https://doi:10.1518/001872099779591231

2. M. A. Lafortune, E. M. Hennig, Cushioning properties of footwear during walking: accelerometer and force platform measurements, Clin. Biomech. 7(3) (1992) 181–184, https://doi.org/10.1016/0268-0033(92)90034-2

3. M. Campbell, T. X. Us, Patent Application Publication (10) Pub (2015), No: US 2015 / 0176237 A1

4. G. N. Greaves, A. L. Greer, R. S. Lakes, T. Rouxel, Poisson's ratio and modern materials, Nat. Mater. 10 (2011) 823–37, https://doi.org/10.1038/nmat3134

5. K. E. Evans, A. Alderson, Auxetic materials: functional materials and structures from lateral thinking. Adv. Mater. 12 (2000) 617. https://doi.org/10.1002/(SICI)1521-4095(200005)12:9%3C617::AID-ADMA617%3E3.0.CO;2-3

6. W. Jiang, X. Ren, S. L. Wang, X. G. Zhang, X. Y. Zhang, C. Luo, Y. M. Xie, F. Scarpa, A. Alderson, K. E. Evans, Manufacturing, characteristics and applications of auxetic foams: A state-of-the-art review, Composites Part B: Engineering. 235 (2022), https://doi.org/10.1016/j.compositesb.2022.109733.

7. R. Critchley, I. Corni, J. A. Wharton, F. C. Walsh, R. J. Wood, K. R. Stokes, The preparation of auxetic foams by three-dimensional printing and their characteristics, Adv Eng Mater. 15 (10) (2013) 980–5, https://doi.org/10.1002/adem.201300030

8. R. Lakes, Foam structures with a negative Poisson's ratio, Science. 235 (1987) 1038–40, https://doi.org/10.1126/science.235.4792.1038

9. D. Fan, M. Li, J. Qiu, H. Xing, Z. Jiang, T. Tang, Novel method for preparing auxetic foam from closed-cell polymer foam based on the steam penetration and condensation process, ACS Appl Mater Interfaces. 10 (2018)22669–77, https://doi.org/10.1021/acsami.8b02332

10. F. Chiang, Manufacturing and characterization of an auxetic composite, Supplemental proceedings: materials processing and interfaces, TMS, editor, 2012.

11. N. Chan, K. E. Evans, Fabrication methods for auxetic foams, J Mater Sci. 32(1997) 5945–53, https://doi.org/10.1023/A:1018606926094

12. E. A. Friis, R. S. Lakes, J. B. Park, Negative Poisson's ratio polymeric and metallic foams, J Mater Sci. 23(1988) 4406–14, https://doi.org/10.1007/BF00551939

13. N. H. Z. Abedini, A. Nourani, M. Mohseni, N. Hosseini, S. Norouzi, P. R. Bakhshayesh, Effects of geometrical and processing parameters on mechanical properties of auxetic polyurethane foams. SN Appl. Sci. 162 (2022), https://doi.org/10.1007/s42452-022-05042-8

14. R. S. Lakes, K. Elms, Indentability of Conventional and Negative Poisson's Ratio Foams, J. Compos. Mater. 27(12) (1993) 1193–1202, https://doi.org/10.1177/002199839302701203

15. C. Moroney, A. Alderson, T. Allen, M. Sanami, P. Venkatraman, The Application of Auxetic Material for Protective Sports Apparel, Proceedings. 2(6) (2018) 251, https://doi.org/10.3390/proceedings2060251

16. T. Allen, O. Duncan, L. Foster, T. Senior, D. Zampieri, Edeh, V., and Alderson, A., Snow Sports Trauma and Safety, In Snow Sports Trauma and Safety, I. Scher, R. Greenwald, N. Petrone, Springer, Cham, 2017

17. M. Sanami, N. Ravirala, K. Alderson, A. Alderson, Auxetic materials for sports applications, Procedia Eng. 72 (2014) 453–458, https://doi.org/10.1016/j.proeng.2014.06.079

18. L. A. Stojmanovski Mercieca, C. Formosa, J. N. Grima, N. Chockalingam, R. Gatt, A. Gatt, On the Use of Auxetics in Footwear: Investigating the Effect of Padding and Padding Material on Forefoot Pressure in High Heels, Phys. Status Solidi Basic Res. 254(12) (2017) 1–5, https://doi.org/10.1002/pssb.201700528

19. E. P. Application, Designated extension states, Office, 1(19) (2007)1–18

20. A. Hinrichs, K. Malukhina, I. Sharma, M. Vierra, Active Auxetic Heel Support for Achilles Tendon Therapy, Bioeng. Sr. Theses. (2018), https://doi:10.3390/ma15041439

21. M. R. Dehaghani, A. Nourani, N. Arjmand, Effects of auxetic shoe on lumbar spine kinematics and kinetics during gait and drop vertical jump by a combined in vivo and modeling investigation, Sci Rep. 12(1) (2022) 18326, https://doi.org/10.1038/s41598-022-21540-6

22. A. Cappozzo, Gait analysis methodology. Hum Mov Sci. 3 (1984) 27–50, https://doi.org/10.1016/0167-9457(84)90004-6

23. A. A. Hulleck, M. D. Menoth, N. Abdallah, M. El Rich, K. Khalaf, Present and future of gait assessment in clinical practice: Towards the application of novel trends and technologies, Front

Med Technol. 16 (2022) 901331, https://doi.org/10.3389/fmedt.2022.901331. PMID: 36590154; PMCID: PMC9800936

24. P. R. Cavanagh, Plantar soft tissue thickness during ground contact in walking, J. Biomech. 32(6) (1999) 623–628, https://doi.org/10.1016/s0021-9290(99)00028-7

25. W. R. Ledoux, J. J. Blevins, The compressive material properties of the plantar soft tissue, J. Biomech. 40(13) (2007), 2975–2981, https://doi.org/10.1016/j.jbiomech.2007.02.009

26. N. Mills, Running shoe materials, In Materials in Sports Equipment, M. Jenkins., Woodhead, 2003.

27. Y.T. Jamshidi, S. Sadeghnejad, M. Sadighi, Viscoelastic Behavior Determination of EVA Elastomeric Foams using FEA, The 23rd Annual International Conference on Mechanical Engineering, ISME (2015), http://dx.doi.org/10.13140/2.1.2288.4166

28. G. W. Jenkins, C. P. Kemnitz, G. J. Tortora, Anatomy and physiology: from science to life, 2nd ed., John Wiley and Sons, 2006

29. I. Chowdhury, S. P. Dasgupta, Computation of Rayleigh damping coefficients for large systems, Electron. J. Geotech. Eng., 8(2003) 1–11, https://doi.org/10.1007/s42452-020-2629-z

30. A. I. Yusuf, N. M Amin, Determination of Rayleigh damping coefficient for natural damping rubber plate using finite element modal analysis, InCIEC (2014) 713–725, http://dx.doi.org/10.1007/978-981-287-290-6_62

31. S. Robbins, E. Waked, Balance and vertical impact in sports: Role of shoe sole materials, Arch. Phys. Med. Rehabil. 78(5) (1997) 463–467, https://doi.org/10.1016/s0003-9993(97)90157-x